Journal of Vertebrate Paleontology

Publication details, including instructions for authors and subscription information:
http://www.tandfonline.com/loi/ujvp20

Machairodus aphanistus (Felidae, Machairodontinae, Homotherini) from the late Miocene (Vallesian, MN 10) site of Batallones-3 (Torrejón de Velasco, Madrid, Spain)

Marcos F. G. Monescillo[a], Manuel J. Salesa[a], Mauricio Antón[a], Gema Siliceo[a] & Jorge Morales[a]

[a] Departamento de Paleobiología, Museo Nacional de Ciencias Naturales—CSIC C/José Gutiérrez Abascal, 2. 28006, Madrid, Spain
Published online: 06 May 2014.

PLEASE SCROLL DOWN FOR ARTICLE

MACHAIRODUS APHANISTUS (FELIDAE, MACHAIRODONTINAE, HOMOTHERINI) FROM THE LATE MIOCENE (VALLESIAN, MN 10) SITE OF BATALLONES-3 (TORREJÓN DE VELASCO, MADRID, SPAIN)

MARCOS F. G. MONESCILLO, MANUEL J. SALESA,* MAURICIO ANTÓN, GEMA SILICEO, and JORGE MORALES
Departamento de Paleobiología, Museo Nacional de Ciencias Naturales—CSIC C/José Gutiérrez Abascal, 2. 28006, Madrid, Spain,
marcosfg84@gmail.com; msalesa@mncn.csic.es; mfanton@terra.es; siliceo@mncn.csic.es; mcnm166@mncn.csic.es

ABSTRACT—In the present work we conduct a comparative study of the cranial and dental samples of the early machairodontine *Machairodus aphanistus* from the Vallesian (MN 10) sites of Batallones-1 and Batallones-3 (Torrejón de Velasco, Madrid, Spain). These sites, which have yielded the most abundant and complete samples of this felid, show interesting differences in faunal composition and age, thus providing a unique opportunity for both qualitative and quantitative comparisons between two populations of the same species. The study reveals differences in a number of cranial features, and statistically significant differences in teeth size and proportions. Although probably not enough to support a separation at the species level, these observations fit well with the morphological evolution of the lineage leading towards more derived forms such as the Turolian *Amphimachairodus giganteus*.

INTRODUCTION

'El Cerro de los Batallones' or Batallones Butte is located in the municipality of Torrejón de Velasco, within the Madrid Basin, between the Jarama River and the Prados-Guatén Depression. The UTM (Universal Transverse Mercator) coordinates are 44°47′57″ latitude and 43°92′20″ longitude (Fig. 1). Batallones Butte is one of the 'monadnocks' or 'inselbergs' originated on silicified carbonates on lacustrine carbonate and silicified materials of the lower Vallesian within Miocene Intermediate Unit in the Madrid Basin (Morales et al., 2008). The geologic cartography and the facies analysis of the materials exposed in the quarries in the area of the Batallones Butte allow us to distinguish three lithological units: (I) magnesic bentonitic lutites; (II) sepiolitic lutites and opals; and (III) carbonate, loam, and siliciclastic sediments (Calvo et al., 2013). These three units progress from a lacustrine shore with edaphic palustrine deposits to finally lacustrine-palustrine sediments of fresh water (Pozo et al., 2004). As indicated by Calvo et al. (2013) and Morales et al. (2008), the deposits with vertebrate remains could be considered as a fourth lithological unit, whose facies are similar to those of unit III, but younger in age. The Butte is known since the mid-1980s due to the presence of commercially exploitable deposits of sepiolite (Leguey et al., 1985), but it was not until 1991 that the first site (Batallones-1) was found during mining works carried out by the company Tolsa S.A. (Morales et al., 2008). Up to the present, nine fossil sites have been located in the area, all dated as Late Vallesian in age (MN 10, ca. 9.5 Ma). The principal factor leading to the formation of the fossil sites is thought to be a pseudokarstic process known as 'piping,' which produced a series of cavities in the levels of sepiolite through a 'chambering' process (Pozo et al., 2004). These cavities acted as natural traps for the surrounding fauna, mainly carnivorans that were attracted by the presence of other trapped animals (Antón and Morales, 2000; Pozo et al., 2004; Morales et al., 2008). Thus, in both Batallones-1

and Batallones-3, around 98% of the excavated fossils belong to the Carnivora.

Among these carnivorans, Batallones-1 and Batallones-3 have yielded an abundant sample of remains of the homotherin felid *Machairodus aphanistus*, with several skulls, mandibles, and postcranial elements representing at least 15 individuals in Batallones-1 and 5 individuals in Batallones-3. *Machairodus aphanistus* is a relatively primitive member of the Homotherini, characterized by few and moderately developed machairodont features, mainly laterally flattened and crenulated upper canines (scimitar-toothed), of moderate length, relatively large carnassial teeth, dorsally displaced jugular process, and slightly vertical mandibular symphysis, with the presence of a very small lateral flange. Later genera of this tribe, such as *Amphimachairodus*, *Lokotunjailurus*, *Xenosmilus*, and *Homotherium*, developed derived morphologies from this primitive pattern. In fact, the Turolian species *Amphimachairodus giganteus* already shows enough differences from the Vallesian *M. aphanistus* to be classified in a different genus, as proposed by several authors (Kretzoi, 1929; de Beaumont, 1975; Roussiakis, 2002; Antón et al., 2004; Sardella and Werdelin, 2007).

Although Batallones-1 and Batallones-3 are only separated by around 160 m, their sediments lack any stratification, which prevents any stratigraphic correlation between both localities. Nevertheless, López-Antoñanzas et al. (2010) in their study on the cricetid *Hispanomys moralesi* from some of the Batallones sites indicated that Batallones-3 is younger than Batallones-1, because the former population showed a number of derived features in its dentition in relation to the morphology observed in the Batallones-1 sample. Unfortunately, with these morphological data the exact chronological separation between both localities is difficult to assess. Also, there are important faunal differences between both localities, such as the presence in Batallones-3 of the ursid *Indarctos arctoides*, the large mustelid *Eomellivora piveteaui*, and the amphicyonid *Thaumastocyon* sp. (Salesa et al., 2010, 2012; Abella, 2011; Valenciano et al., 2012), all absent in Batallones-1. Machairodontine felids are the most abundant taxa in both localities, but they show differences in their relative abundance: the leopard-sized saber-toothed felid
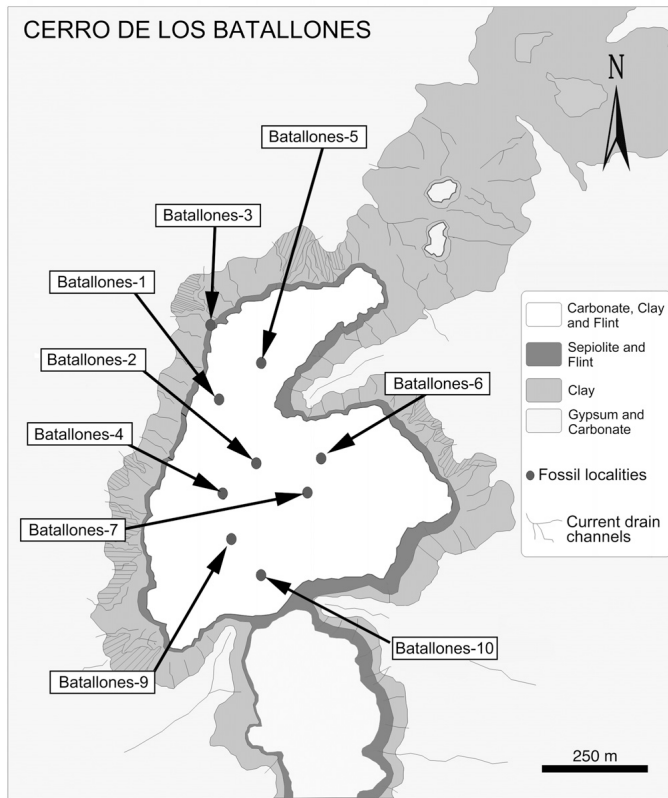
---

*Corresponding author.

FIGURE 1. Schematic map of 'Cerro de los Batallones' in the Madrid Basin, showing the location of the nine sites found, and the geologic levels found. Torrejón de Velasco, Comunidad de Madrid, Spain.

Promegantereon ogygia is the most abundant species in Batallones-1 (Antón and Morales, 2000; Salesa, 2002), followed by *M. aphanistus,* whereas in Batallones-3, *M. aphanistus* and *I. arctoides* are more abundant than *P. ogygia* (Abella, 2011; Siliceo et al., 2011). Thus, the relative abundance of the two large felids is reversed in Batallones-1 and Batallones-3, which could imply a difference in their population densities between both communities, and thus paleoecological differences, suggested as well by the mentioned presence/absence of other large carnivorans. In

the present study on the craniodental morphology of *M. aphanistus* from Batallones-1 and Batallones-3, we found size differences in the skull, and statistically significant differences in teeth size and proportions, which indicate that the mentioned chronological disparity was important enough to produce a slight morphological separation between both populations. Thus, although these differences are probably not strong enough to support a species separation, they fit with the morphological evolution of the lineage leading to more derived forms of homotherins, such as the Turolian *A. giganteus.*

MATERIALS AND METHODS

Material

The studied fossil sample is housed at the collections of the Museo Nacional de Ciencias Naturales–CSIC, Madrid, Spain. The material resulted from the excavations of 1991–2008 (Batallones-1) and 2005–2011 (Batallones-3), led by Prof. J. Morales.

Methods

The anatomical descriptions follow the terminology used by Barone (2010) and the Nomina Anatomica Veterinaria (2005). The measurements were taken with a 15 mm digital caliper, and with a 500 mm manual precision caliper; they are shown in Figure 2 and in Table 1. Quantitative data were analyzed using Student's t test in the statistic software package IBM SPSS Statistic 19.0. Results are shown in Table 2. The requirements of the Student's t test are a normal distribution of data and the existence of homoscedasticity, which was checked using the Levene test. In the cases with heteroscedasticity, the conservative Welch test was used to check for equal means, instead of the Student's t test.

The MNI (minimum number of individuals) was estimated on the basis of adult cranial, mandibular, and dental materials, and was 15 for Batallones-1 and 5 for Batallones-3. The sexual dimorphism index was estimated using the 'mean method' of Plavcan (1994) and Van Valkenburgh and Sacco (2002). This method was applied to the four most dimorphic measurements, which are the basal length of the skull, the mesiodistal length of the upper canine, the buccolingual width of the upper canine, and the mesiodistal length of m1 (Table 3). Finally, in order to maintain the independence of the data between the two populations, where there were two of the same element from the same individual (for example, both right and left P4 in the same skull), we took the average measurement of both.
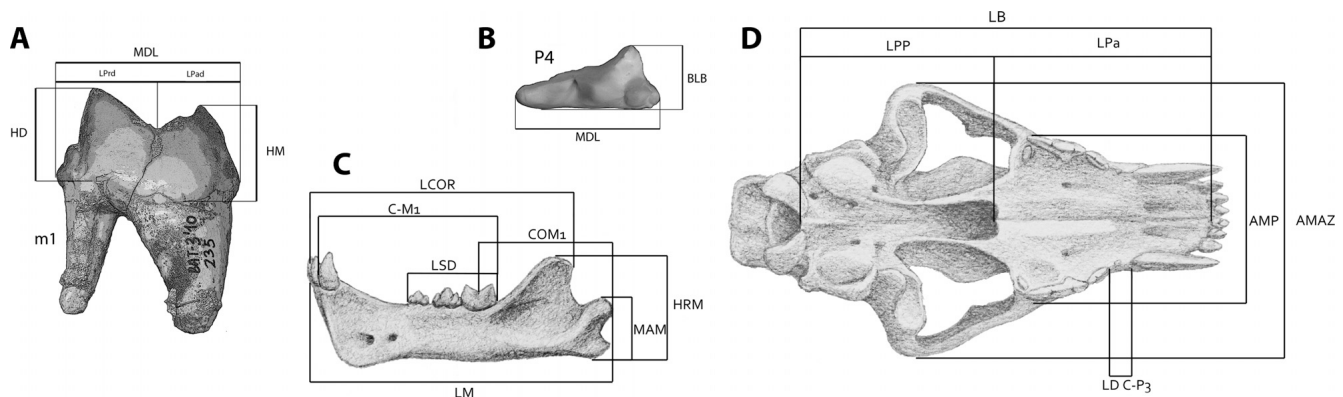

FIGURE 2. Measurements for each studied cranial, mandibular, and dental elements. **A**, labial view of the m1; **B**, oclusal view of the P4; **C**, labial view of the mandible; **D**, ventral view of the skull.

Institutional Abbreviations—**BAT-1**, **B**, Batallones-1; **BAT-3**, Batallones-3; **B/S**, Batallones-1, fossil not found in situ; **MNCN**, Museo Nacional de Ciencias Naturales–CSIC.

Anatomical Abbreviations—**C**, upper canine; **c**, lower canine; **I**, upper incisor; **i**, lower incisor; **P**, upper premolar; **p**, lower premolar **m**, lower molar; **M**, upper molar.

Measurements and Statistical Abbreviations—**AMAZ**, maximum zygomatic arch width; **AMP**, maximum maxilla width; **BLW**, buccolingual width; **C–M1**, length from the caudal edge of the m1 to the rostral canine edge; **COM1**, length from the condylar process caudal edge to notch between the protoconid and paraconid of the m1; **H**, crown tooth height; **HD**, m1 protoconid height; **HM**, m1 paraconid height; **HRM**, height from the ventral edge of angular process to dorsal edge of the coronoid process; **LCOR**, mandibular length from the caudal edge of the coronoid process to the rostral mandibular edge; **LB**, basal skull length; **LD C–P3,** diastema between upper canine and upper third premolar; **LM**, mandibular length; **LPa**, length from the rostral edge of incisive bone to the caudal edge of maxilla bone; **LPad**, paraconid length; **LPP**, length from the caudal edge of the maxilla bone to the caudal edge of the foramen magnum; **LPrd**, protoconid length; **LSD**, dental sequence length; **MAM**, height from the ventral edge of angular process to the dorsal edge of the condylar process; **MDL**, mesiodistal length; **SD**, standard deviation.

<div align="center">

SYSTEMATIC PALEONTOLOGY

Class MAMMALIA Linnaeus, 1758
Order CARNIVORA Bowdich, 1821
Suborder FELIFORMIA Kretzoi, 1945
Family FELIDAE Fischer, 1817
Subfamily MACHAIRODONTINAE Gill, 1872
Genus *MACHAIRODUS* Kaup, 1833
MACHAIRODUS APHANISTUS (Kaup, 1832)
(Figs. 3–7)

</div>

Referred Material—Batallones-1: B-2706, skull with mandible showing P3 and P4 and broken right upper and lower canines; B-4711, skull with right C, I3, and P3–M1, and left C and P3–M1; B-5445, skull and mandible with right P4 and P3, and left C, p4, and m1; BAT-1'05 E6-42, skull with right I3–P4, and left I3–P4; BAT-1'07 F4-77, skull with right I3, C, and P4, and left C and P4; B-6046, skull with right P3 and P4, and left P4 and M1; B-4151 (1), skull with right I3, C, and P4, and left C and P4; BAT-1'05 F6-314, skull with right C–P4, and left C and P4; B-4272, skull with mandible showing right C, P4, and M1, and left C and P4; B-1523, skull with right C–P4, and left P3–M1; BAT-1'04 E4-200, skull with right and left P4; BAT-1'04 D5-35a, skull and mandible showing right C–P4, and left I3–P4; B-8642, right I3; B-5160, right I3; B-2383, left I3; B-8643, right I3; B-8640, right I3; B-442, left I3; B-8641, left I3; B-4017, left I3; BAT-1'02 E4-111, left I3; B-3797, right C; B-3553, left C; B-4256, right C; B-4963, left C; B-970, right C; B-1392, left C; B-8636, left P3; B-8637, right P3; B-3940, right P3; B-861, fragment of right P3; B-3316, left P3; B-782, left P3; B-512, left P3; B-149, right P3; B-4607, right P4; B-340, left P4; BAT-1'04 F6-130, mandible with right p4 and m1, and left c–m1; BAT-1'06 F6-80, mandible with right c, p4, and m1, and left c–m1; B-2230, mandible with right and left p4; B/S-8-6, mandible with right and left m1; BAT-1'05 F6-265, mandible with right and left p4 and m1; B-8639, mandible with right c, p4, and m1, and left m1; B-382, right hemimandible with p4; B-3974, right hemimandible with m1; B-8644, left hemimandible with p3–m1; B-8630, right hemimandible with c, p4, and partially broken m1; B-293, right c; B-598/2, right c; B-8638, left c; B-2625, right c; B-4025, right c; BAT-1'03 E4-193, right c; BAT-1'02 D4-207, right c; BAT-1'03 D4-337, left c; B-834/11, right c; B-1025, left p3; B-8633, right p3; B-593, right p3; B-8631, right p3; B-8631, right p3; B-8634, right p3; B-3663, right p3; B-3393, right p3; BAT-1'08, C4–3, right p3;

B-268, right p3; B-99 (1), fragment of right p3; B-8644, left p3; B-3702, right p4; B-8635, left p4; B-3271, left p4; B-3899, left p4; B-8649, fragment of right p4.

Batallones-3: BAT-3'05 109, skull with right P4 and left I3; BAT-3'08 606, skull with right and left P4; BAT-3'06 706, skull with right and left P4; BAT-3'09 1622, skull with right I2–C and P4, and left I2–P4; BAT-3'10 785, left I3; BAT-3'09 58, right I3; BAT-3'09 15 left C; BAT-3'07 981, left C; BAT-3'10 635, left C; BAT-3'09-59, left P3; BAT-3'09 89, right P3; BAT-3'10 26, left P4; BAT-3'09 1623, mandible with right c–p4; BAT-3'08 252, left hemimandible with m1; BAT-3'09 1017, mandible with right c; BAT-3'11 370, right c; BAT-3'10 784, left c; BAT-3'10 629, right c; BAT-3'11 774, left p3; BAT-3'11 1204, left p3; BAT-3'09 166, right p3; BAT-3'10 719, right p4; BAT-3'11 2032, left p4; BAT-3'10 149, right p4; BAT-3'08 92, left p4; BAT-3'10 235, right m1, BAT-3'08 252, left m1; BAT-3'08 1207, left m1.

<div align="center">

DESCRIPTION AND COMPARISONS

</div>

The material from Batallones-1 was described by Antón et al. (2004), so here we only provide a full description of that from Batallones-3.

Cranium—Most of the skulls from Batallones-3 are severely damaged and eroded, their state of preservation being poorer than in Batallones-1. In dorsal view (Fig. 3B), the skull of *M. aphanistus* from Batallones-3 is relatively narrower and slenderer than that of a similarly sized pantherin felid such as *Panthera leo*; this is evident when comparing the nasals, the frontal bone, the zygomatic arches, and the parietal region. The premaxilla is slightly expanded rostrally, showing a moderately procumbent incisive row (Fig. 3D). The nasal bones are broadly rectangular, with straight caudal borders, whereas in the pantherins they are triangular, with caudally extended caudal borders; in both cases there is a slight depression in the caudal part of the nasal suture (Fig. 3B). The right and left temporal lines meet dorsally at the level of the external auditory meatus, continuing in a strong and long sagittal crest. The infraorbital foramen is relatively large and located at the level of P3. The lacrimal foramen is located in the inner face of the rostral border of the orbit. In ventral view, the incisor arcade has a gentle curvature, much less rostrally extended than that of derived machairodontines. The tympanic bullae are elliptic, and they appear as inflated as those of a pantherin felid, extending from the rostral margin of the jugular process to the caudal margin of the postglenoid process, without contacting with the latter. The caudal entotympanic penetrates rostrally beside the medial margin of the ectotympanic. The external auditory meatus is a single opening, rostrolaterally oriented. In lateral view, the incisor row is rostrally prominent and slightly curved, but to a lesser degree than that of derived machairodontines. The premaxilla is markedly inflated due to the large canine root. The zygomatic arch is relatively long and straight, such as that of pantherins, thus differing from the shorter and dorsally curved arch of derived machairodontines. The sagittal crest is caudally elongated, showing a convex dorsal profile, more curved than those of pantherins, due to the more inclined occipital of *M. aphanistus* (Fig. 3A–C). The nuchal crest is straight and rostroventrally oriented. The jugular and mastoid processes are located almost at the same level, as in the skulls from Batallones-1, in an intermediate state between those of pantherins (with a jugular process located ventrally to the mastoid process) and derived machairodontines (with a very reduced jugular process located dorsally to the mastoid process). In rostral view, the orbits are relatively smaller than those of pantherins and the rostrum shows an intermediate morphology between the narrower and square-shaped muzzle of derived machairodontines and the broad and heart-shaped one of the pantherin cats. The frontal process of the zygomatic is moderately developed, with a sharp dorsal edge, and caudodorsally projected, whereas the zygomatic process of the frontal is very
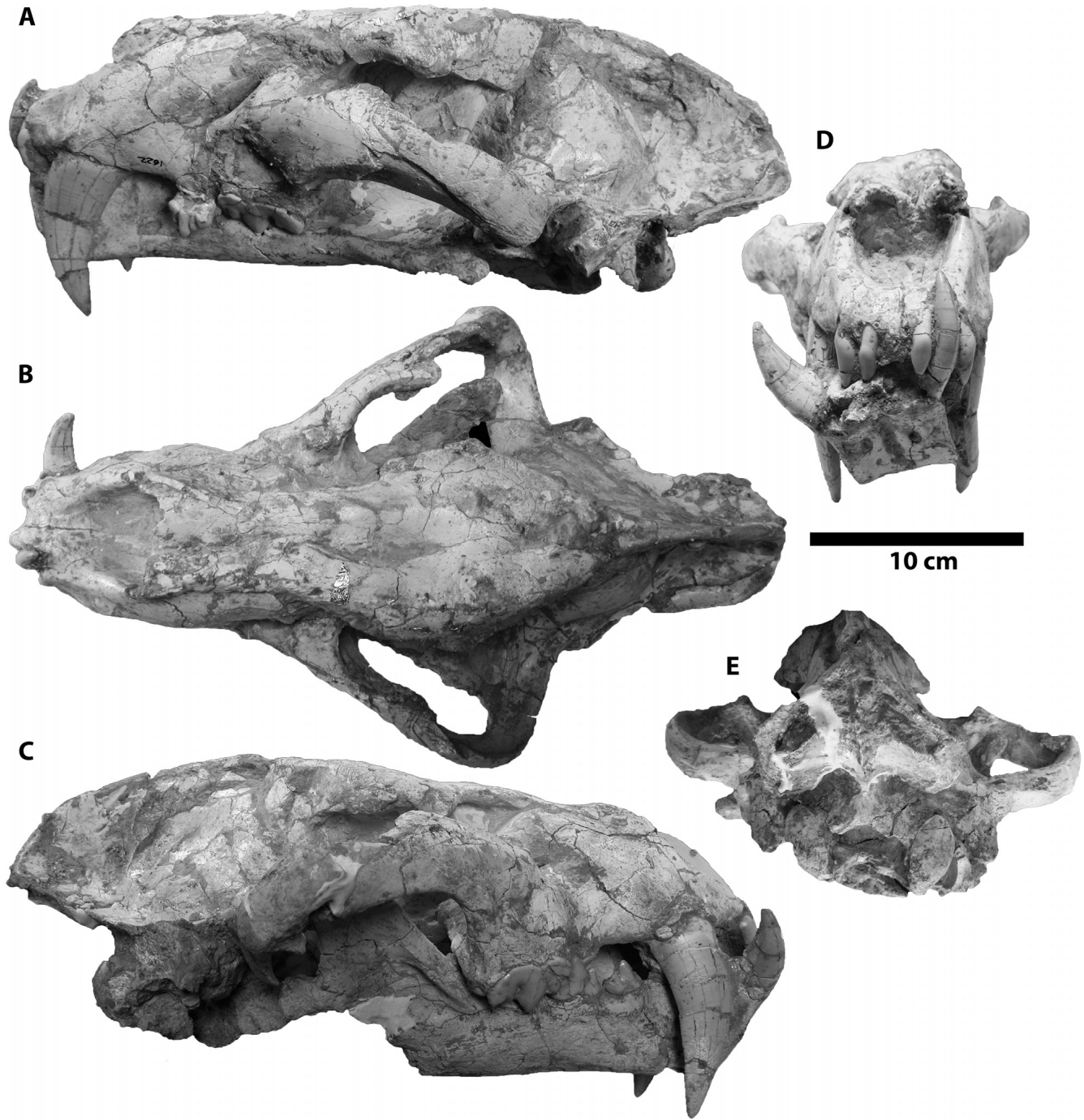
FIGURE 3. Skull and mandible of *Machairodus aphanistus* from Batallones-3. **A–E**, skull (BAT-3'09 1622) and mandible (BAT-3'09 1623) in **A**, left lateral view; **B**, dorsal view; **C**, right lateral view; **D**, rostral view; **E**, caudal view.

reduced and rough. In caudal view, the occipital external crest is located in the sagittal plane, and surrounded by deep depressions (Fig. 3E). The nuchal crests define the external limits of the upper occipital region. The occipital condyle and the foramen magnum are similar in relative size to those of a pantherin.

Upper Dentition—The incisors are mostly caniniform, with the I3 being much larger than I1 and I2, which show a similar size. The upper incisor roots are laterally flattened and shorter than those of the lower incisors. The I2 crown is laterally compressed and slightly distally curved; it has two lingually located accessory cusps. The I3 is strongly caniniform, with a sharp main cusp, and a mesiolingual accessory cusp; the main cusp has two crenulated edges (observable in the best preserved specimens), one running buccomesially, and the other linguodistally; the root is robust and rounded, with a blunt and wide apex. The upper canines are very elongated, with laterally flattened and distally curved crowns showing strong crenulations in both distal and mesial borders. Two upper canine 'morphotypes,' independent from size, seem
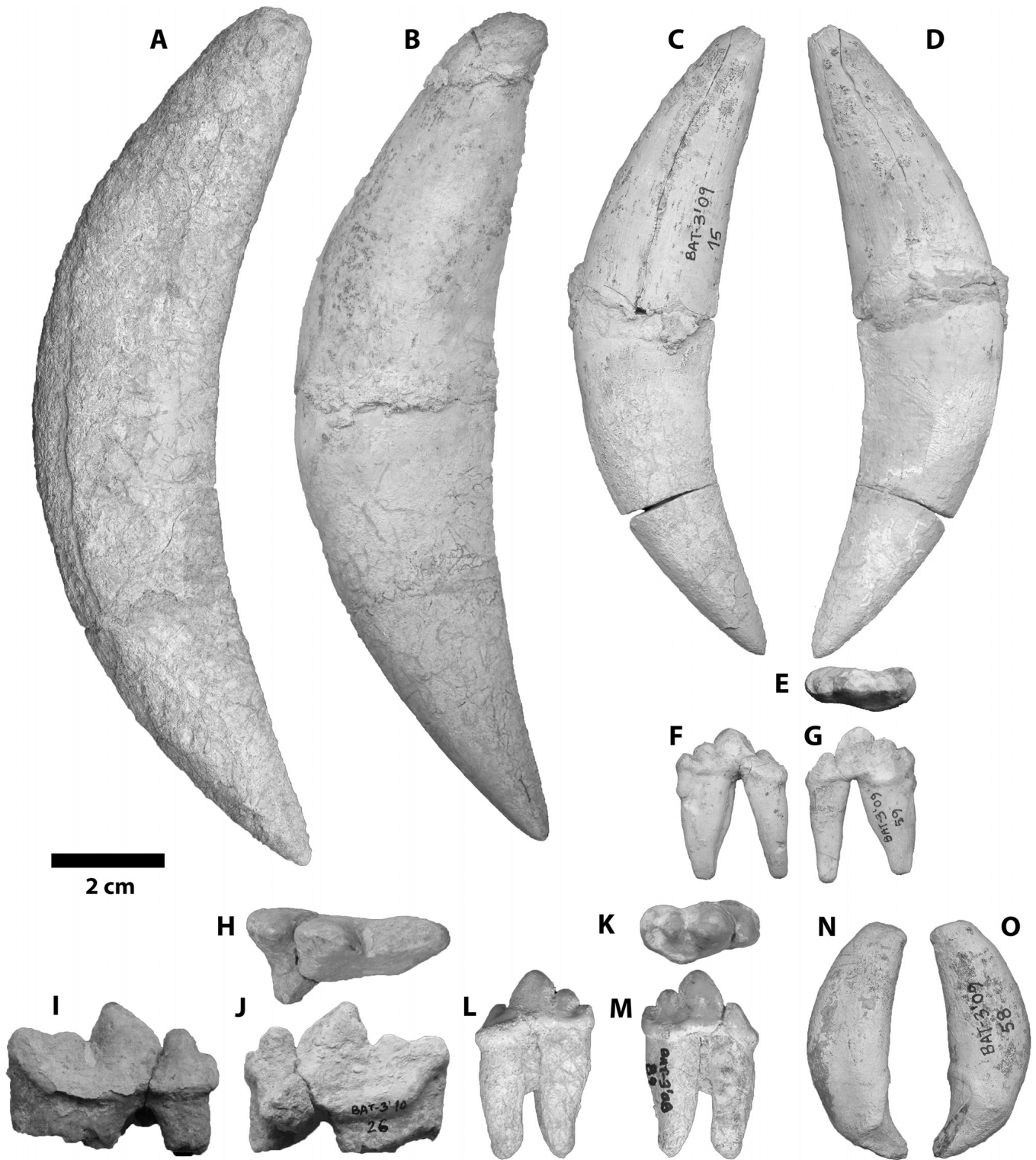
FIGURE 4. Upper teeth of *Machairodus aphanistus* from Batallones-3. **A**, left upper canine (BAT-3'07 981 15) in labial view; **B**, left upper canine (BAT-3'09 82) in labial view; **C**, **D**, left upper canine (BAT-3'09 15) in **C**, labial view; **D**, lingual view; **E**–**G**, left P3 (BAT-3'09 59) in **E**, oclusal view; **F**, labial view; **G**, lingual view; **H**–**J**, left P4 (BAT-3'10 26) in **H**, oclusal view; **I**, labial view; **J**, lingual view; **K**–**M**, right P3 (BAT-3'09 89) in **K**, oclusal view; **L**, labial view; **M**, lingual view; **N**, **O**, right I3 (BAT-3'09 58) in **N**, mesial view; **O**, caudal view.
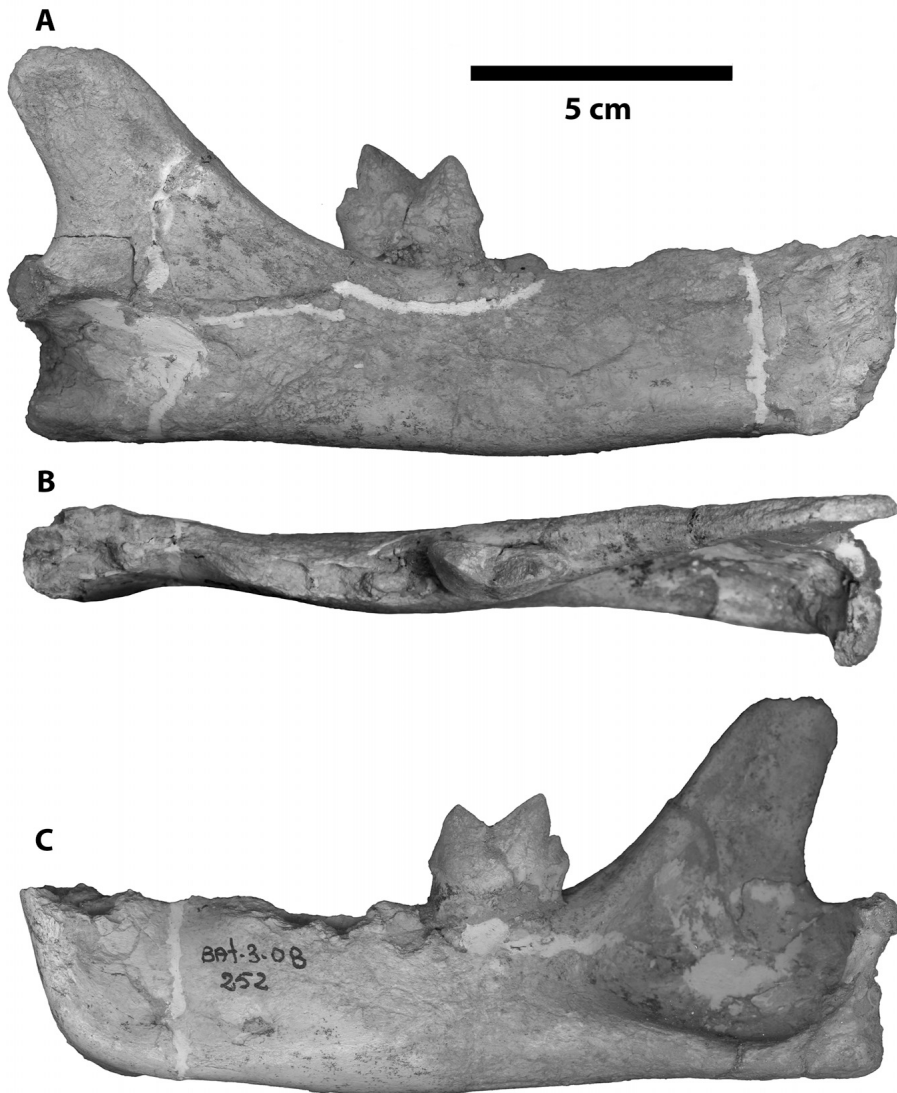
FIGURE 5. Left hemimandible of *Machairodus aphanistus* from Batallones-3. **A–C**, left hemimandible (BAT-3'08 252) in **A**, medial view; **B**, occlusal view; **C**, lateral view.

to be present within the sample, because some specimens are relatively mesiodistally longer than others (Fig. 4A, B). The P3 has a large main cusp, and two similarly sized mesial and distal cusps; there is also a distal cingulum, ended in a little tip (Fig. 4E–G, K–M). The main cusp is lightly crenulated, and higher than the other cusps; the mesial cusp is the lowest. In oclusal view, the P3 may have a distolingual protuberance, highly variable in the Batallones-3 specimens, and much more homogeneous in the sample from Batallones-1; this feature produces strong differences in the buccolingual width of the P3 from Batallones-3; the lingual edge of the crown is mainly convex, whereas the labial one is concave; both roots are slightly lingually sloped, with vertical grooves on their lingual sides, much more marked in the distal root; the mesial root is conical, and more gracile than the distal one. The P4 (Fig. 4H–J) has a very reduced, lingually oriented protocone, located between the parastyle and paracone; there is a small crest connecting protocone with paracone. The parastyle is well developed, and there is a small, slightly buccally located ectostyle. The metacone-metastyle edge is slightly longer than the paracone, with a marked notch separating both struc-

tures; there is no cingulum; there are three roots, the larger one, laterally flattened, corresponding to the paracone-mestastyle; the other two roots are more or less conical. The M1 is highly reduced, possessing an elliptic, very low crown, with a gentle buccolingual crest and no observable cusps.

Mandible—In lateral view (Fig. 5C), the dorsoventral height is almost constant along the mandibular corpus. The ventral edge is mostly straight or slightly concave, whereas in large pantherins it is concave, and convex in derived machairodontines. As Antón et al. (2004) indicated, the symphyseal area is more vertical than in pantherins, but less vertical than in derived machairodontines. There are two mental foramina, the larger one being located at the level of the postcanine diastema, and the smaller one being placed just below the p3. In rostral view, the symphyseal area is rectangular and relatively higher than in pantherins, showing a small, ventrally expanded mental crest; furthermore, the rostral edge is laterally widened, with marked mental crests (Figs. 3D, 5A–C). On the medium symphyseal line, a vertical groove, less marked than in derived machairodontines, is observed, which continues on the ventral edge (Fig. 3D). In ventral view, as in
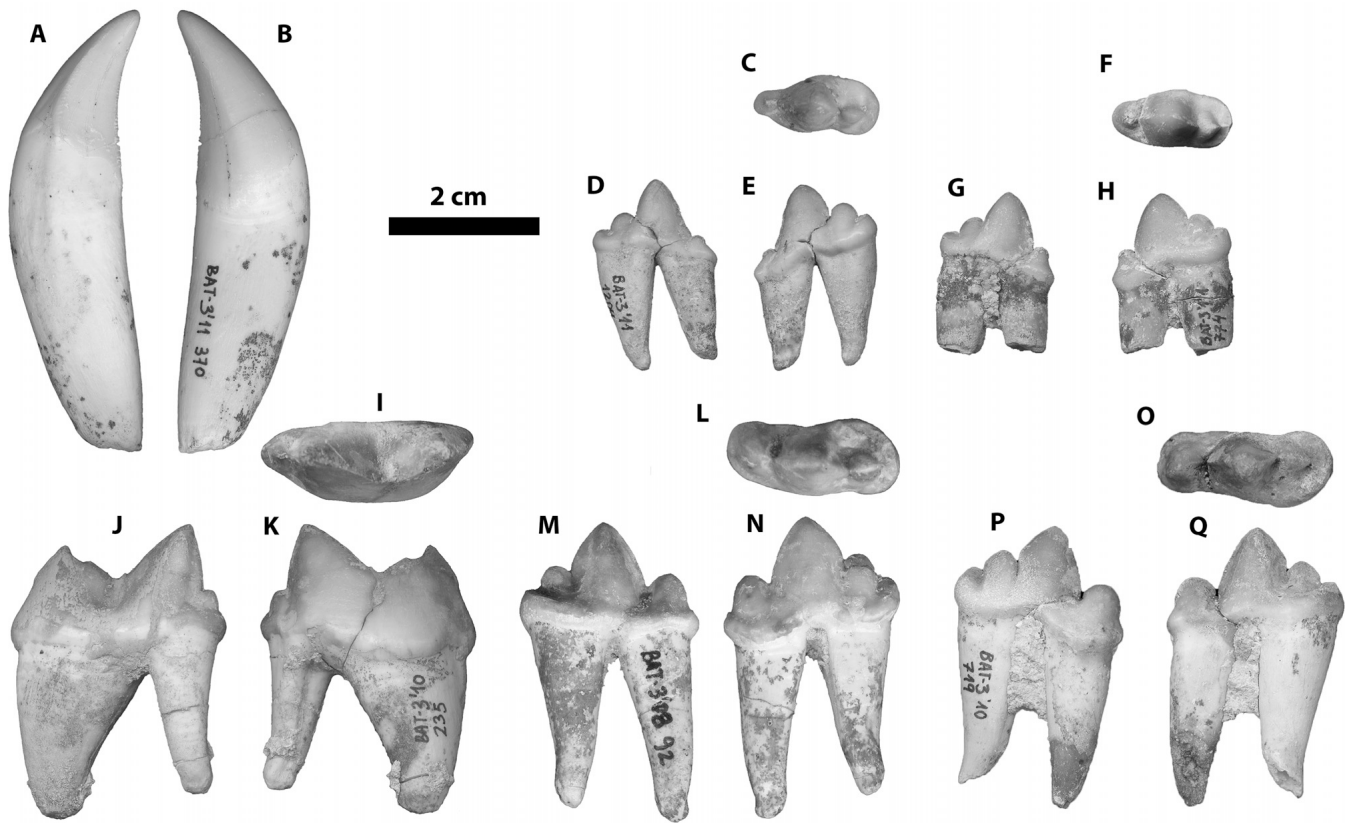
FIGURE 6. Lower teeth of *Machairodus aphanistus* from Batallones-3. **A**, **B**, right lower canine (BAT-3'11 370) in **A**, lingual view; **B**, labial view; **C–E**, left p3 (BAT-3'11 1204) in **C**, oclusal view; **D**, lingual view; **E**, labial view; **F–H**, left p3 (BAT-3'11 774) in **F**, oclusal view; **G**, lingual view; **H**, labial view; **I–K**, right m1 (BAT-3'10 235) in **I**, oclusal view; **J**, lingual view; **K**, labial view; **L–N**, left p4 (BAT-3'08 92) in **L**, oclusal view; **M**, lingual view; **N**, labial view; **O–Q**, right p4 (BAT-3'10 719) in **O**, oclusal view; **P**, labial view; **Q**, lingual view.

Batallones-1 (Antón et al., 2004), the symphyseal area does not extend caudally nearly as much as in pantherins, thus resembling *A. giganteus* and other machairodontines. The masseteric fossa is as deep as that of pantherins; its rostral edge is variable, reaching in some cases the level of the m1 protoconid. The coronoid process, similarly sized as those of large pantherins, has a more round caudodorsal tip than the latter. The dorsal edge of the coronoid process is at the level of the caudal edge of the condylar process. The caudal edge of the angular process does not surpass the level of the condylar process. In caudal view, the angular process is rough and medially inclined, with a wide dorsal groove that continues rostrally; this is also observed in *A. giganteus*, whereas in large pantherins the angular process is round in cross-section, and more robust medially. The condylar process is cylindrical, with a laterally located apex; its ventral edge is slightly sloped medioventrally. In medial view, the mandibular foramen is similar in development and location to that of pantherins and *A. giganteus*.

Lower Dentition—The incisors are quite caniniform, with i3 being the largest one, then i2 and finally i1. The roots of the lower incisors are slightly distomesially flattened, and larger and thinner than those of the upper ones. The i3 crown is pointed, lingually curved, mesiodistally elongated, with a small accessory cuspid, mesially located. The lower canine is laterally flattened, but not so much as the upper canine (Fig. 6A, B); its crown, robust, and distolingually curved, is between 1/3 and 1/2 of the total tooth length, showing marked crenulations. When placed in the alveolus, the lower canine is located with its longitudinal

axis parallel to the vertical axis of the symphysis; therefore, the crown tip becomes lingually oriented. Although some specimens from Batallones-1 show a small alveolus for p2 (Antón et al., 2004), no trace of this has been found among the material from Batallones-3. The p3 has three well-developed cuspids and a small distal cingulum (Fig. 6C–H); the main cusp is the higher one, and it shows a certain degree of width variability; the height of the mesial cuspid is very variable, ranging from being very small to similar in size to that of the distal cuspid. In occlusal view, the distal half of the crown is wider than the mesial one; both roots are conical, with longitudinal lingual grooves; the distal root is longer and wider than the mesial one. The p4 (Fig. 6L–Q) is similar in shape to the p3, but it is more robust and larger, and its mesial cusp is relatively larger than that of p3, and more similar in height to the distal one. The distal cingulum of p4 is marked, more so than that of p3, and ends distally in a small point. The roots are conical, ventrally oriented, with the distal one being more robust than the mesial root, both showing a lingual, smooth groove. The m1 has a very reduced metaconid and talonid; the protoconid is slightly higher and mesiodistally longer than the paraconid, with a marked notch separating them (Fig. 6I–K); in occlusal view, both lingual and labial borders are concave, the latter being markedly curved, whereas the lingual border is nearly flat; the mesial root, located under the paraconid and half of the protoconid, is wider and more robust than the distal one; the distal root is located below part of the protoconid and the metaconid, and is conical and narrow.

Tooth measurements are summarized in Table 1.

TABLE 1. Summary of the tooth measurements (in mm) of *M. aphanistus* from Batallones-1 and Batallones-3.

Locality	Tooth	N	MDL		BLM		H	
			Mean	SD	Mean	SD	Mean	SD
BAT-1	C	15	29.85	2.50	12.80	0.92	65.57	6.88
BAT-3	C	6	30.75	4.01	14.08	1.68	72.21	7.07
BAT-1	P3	20	23.62	1.44	11.76	1.01	11.37	0.57
BAT-3	P3	3	22.19	1.50	10.22	1.79	10.28	1.30
BAT-1	P4	24	38.35	2.85	17.89	1.10	17.60	0.93
BAT-3	P4	7	37.15	1.96	17.55	1.31	16.84	2.76
BAT-1	c	15	17.78	1.15	11.34	0.65	29.43	3.54
BAT-3	c	6	17.27	0.96	11.31	0.54	30.22	2.36
BAT-1	p3	15	19.12	0.86	8.73	0.52	10.98	0.51
BAT-3	p3	4	17.88	1.16	8.71	0.20	10.93	0.38
BAT-1	p4	20	25.11	1.38	11.44	0.66	15.48	1.27
BAT-3	p4	5	24.24	1.08	10.64	0.28	14.44	0.81
BAT-1	m1	24	30.46	1.30	13.40	0.74	17.92/17.28*	1.20/1.05*
BAT-3	m1	3	29.58	0.18	11.91	0.47	16.45/17.06*	0.19/0.11*

*First measurement refers to paraconid height; second measurement refers to protoconid height.

DISCUSSION

The statistical analysis of the sample of *M. aphanistus* from Batallones-3 showed that it did not differ significantly in cranial and mandibular measurements from the Batallones-1 sample, but did differs significantly in some dental measurements and indices: H of P3, MDL of p3, BLW of p4, BLW of m1, MDL/BLW of m1, and BLW/HM of m1 (Table 2). A scatterplot of these variables shows that the distribution of the Batallones-3 sample is always located close to the lower values from Batallones-1, in both significant and nonsignificant measurements. A possible explanation for this could be smaller body size for the individuals from Batallones-3 in relation to those from Batallones-1, but could also result from some kind of entrapment bias in favor of small adults (females), or simply reflect the small sample size.

Nevertheless, there are morphological differences between the two populations that deserve a more detailed discussion. The upper canines of both samples do not show significant differences, and the presence of the described 'morphotypes' within Batallones-3 is very interesting, even if a larger sample would be necessary to perform the corresponding statistical tests. The presence of p2 in Batallones-1 and its absence in Batallones-3 could be considered an interesting difference, given the fact that its loss is a derived feature (de Beaumont, 1975; Sotnikova, 1992). Concerning the P3, and although there are no statistical differences between both populations, we did find a strong phenotypic variability within the Batallones-3 sample, which is not observable within the larger and much more homogeneous sample from Batallones-1. This variability is observed in occlusal view, with some specimens having a 'normal' development of the basal distolingual expansion (Fig. 7A–C, 7G–H), and others showing a strong reduction of this structure (Fig. 7D–F). This

difference may seem of little importance, but given the strong reduction of P3 seen in the derived *Amphimachairodus giganteus*, it is remarkable that the P3 from the Batallones-3 shows a higher phenotypic diversity than that of the putatively older population of Batallones-1, indicating that a derived morphology appears alongside the primitive pattern. Finally, the presence in Batallones-3 of relatively narrower, and thus more sectorial, p4 and m1 (Fig. 8) seems to represent another derived trait, although the teeth show an overall morphology very similar to that of Batallones-1, even considering the vestigial talonid of m1. All of these differences indicate the existence of a small but significant morphological separation between the populations of Batallones-1 and Batallones-3, which fits well with the estimated differences in age between these two sites (López-Antoñanzas et al., 2010). It seems clear that the differences are not strong enough to support the existence of two species of *Machairodus* in these localities,

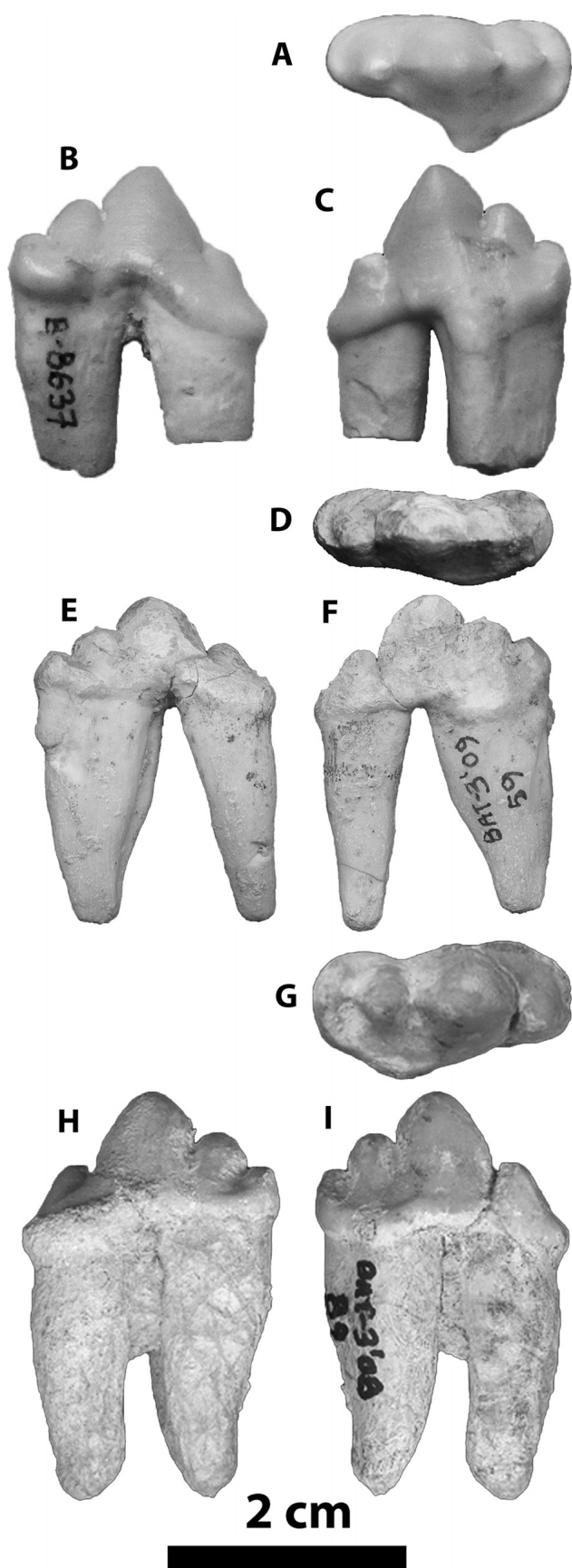TABLE 2. Summarized results of the Student's t tests showing the variables that showed significant differences.

Tooth	Variable	P	Comments
P3	H	0.033	BAT-3 shows lower P3
p3	MDL	0.030	BAT-3 shows shorter p3
p4	BLW	0.046	BAT-3 shows narrower p4
m1	BLW	0.003	BAT-3 shows narrower m1
m1	MDL/BLW	0.001	BAT-3 shows relatively narrower m1
m1	BLW/HM	0.010	BAT-3 shows relatively narrower m1

TABLE 3. Sexual dimorphism index for several species of extant and fossil Felidae.

Species	BL (skull)	MDL (upper C)	BLW (upper C)	MDL (m1)	Average
Caracal caracal	1.08	1.06	1.03	1.08	1.06
Leptailurus serval	1.08	1.10	1.14	0.97	1.07
Smilodon fatalis	1.06	1.09	1.12	1.07	1.09
Panthera onca	1.06	1.12	1.11	1.06	1.09
Puma concolor	1.08	1.14	1.09	1.04	1.09
Acinonyx jubatus	1.10	1.15	1.11	1.09	1.10
Promegantereon ogygia BAT-1	1.09	1.11	1.11	1.09	1.10
Lynx rufus	1.10	1.16	1.11	1.06	1.11
Felis sylvestris	1.10	1.15	1.13	1.08	1.12
Felis chaus	1.07	1.16	1.15	1.10	1.12
Panthera tigris	1.16	1.16	1.08	1.12	1.13
Machairodus aphanistus BAT-1	1.19	1.14	1.14	1.08	1.14
Machairodus aphanistus BAT-3	1.15	1.23	1.26	1.01	1.16
Panthera leo	1.12	1.25	1.23	1.13	1.18
Panthera pardus	1.13	1.24	1.26	1.12	1.19

Data were taken from Salesa (2002) (for *P. ogygia*) and Van Valkenburgh and Sacco (2002) (for the remaining species, except *M. aphanistus* from Batallones-1 and Batallones-3, which were calculated in the present work). Note: *Machairodus aphanistus* has the third highest sexual dimorphism index among the plotted taxa.

← FIGURE 7. Comparison between selected P3 from Batallones-1 and Batallones-3. **A–C**, left P3 from Batallones-1 (B-8637) in **A**, occlusal view; **B**, labial view; **C**, lingual view; **D–F**, left P3 (BAT-3'09 59) from Batallones-3 in **D**, occlusal view; **E**, labial view; **F**, lingual view; **G–I**, right P3 (BAT-3'08 89) from Batallones-3 in **G**, occlusal view; **H**, labial view; **I**, lingual view.

but they herald the morphological changes observed in the more derived, Turolian taxon *A. giganteus*.

PALEOBIOLOGY OF THE CARNIVORAN COMMUNITY FROM BATALLONES-3

The disparity in the faunal composition between Batallones-1 and Batallones-3, with reversed abundance of saber-toothed felids and the presence in the latter site of *Indarctos arctoides*, *Eomellivora piveteaui*, and *Thaumastocyon* sp. (Salesa et al., 2010, 2012; Abella, 2011; Valenciano et al., 2012), absent in Batallones-1, could be indicative of marked habitat and paleoecological differences between these two populations of *M. aphanistus*. For example, the large, hypocarnivorous ursid *I. arctoides* was abundant in Batallones-3, with around 21% of the total bones, and its presence in this site and absence in Batallones-1 could be explained due to either its absence in the central basin of Spain during the formation of Batallones-1, or the existence in Batallones-1 of a more open environment than that of Batallones-3, a habitat probably avoided by this large ursid (Abella et al., 2011). The first possibility is more probable, because the predominance of *Promegantereon ogygia* over *M. aphanistus* in Batallones-1 would imply that the trap was formed in a wooded area, with at least enough vegetation coverage to allow this former species escape from attack by the latter, much larger *M. aphanistus* (Antón and Morales, 2000; Salesa et al., 2006; Turner et al., 2011).

Concerning the observed differences in teeth proportions and canine 'morphotypes' between the two populations of *M. aphanistus*, it is noticeable that these are not related to size, because both populations show similar size and sexual dimorphism indices. In fact, as it has been previously noticed (Antón et al., 2004; Salesa et al., 2006) that *M. aphanistus* exhibits one of the highest sexual dimorphism indices within Felidae (Table 3). The most dimorphic species are leopard and lions, which is very interesting in view of the different breeding system of these two felids. Lions have a very competitive system, with males defending a large group of females (Alderton, 1998; Bothma and Walker, 1999), which seems to explain their high sexual dimorphism index (Bertram, 1979; Van Valkenburgh and Sacco, 2002). On the other hand, male leopards also compete for mates but are largely solitary animals, more so than any other pantherin (Bailey, 1993). This suggests that there is no clear relationship between the sexual dimorphism index and the presence of social systems in Felidae (Van Valkenburgh and Sacco, 2002; Salesa et al., 2006). Also, the low frequency of juvenile individuals within both samples of *M. aphanistus*, with just one specimen in each sample showing milk dentition, suggests that, as among extant felids, the cubs and juveniles were kept apart from the hunting activities, making it highly improbable that they were trapped in the Batallones cavities.

In any case, the most important morphological differences between the samples of *M. aphanistus* from Batallones-1 and Batallones-3 seems to be related to an improved efficiency in resource exploitation. For example, the buccolingually narrower
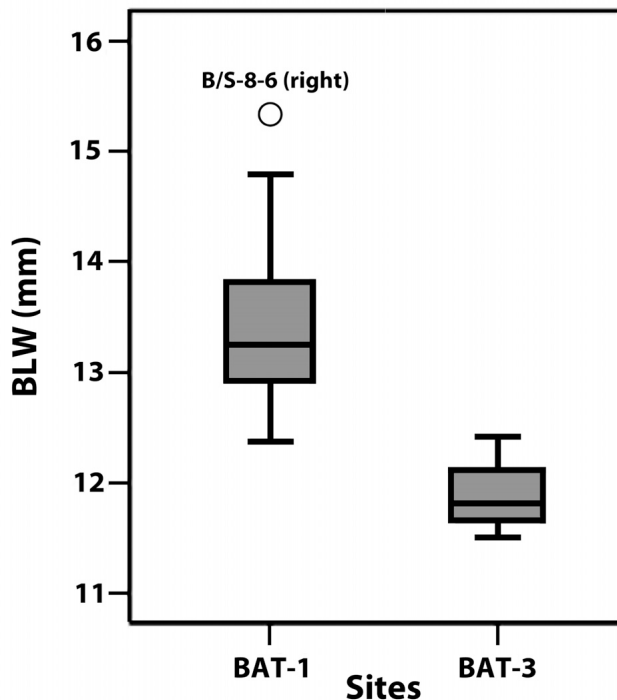
FIGURE 8. Box plot showing the distribution for the values of m1 BLW from Batallones-1 and Batallones-3. The outlier from Batallones-1 corresponds to the fossil B/S-8-6 (right).

p4 and m1 implies a more efficient carnassial blade and thus faster meat consumption. This feature at least indicates some degree of ecological advantage in relation to the Batallones-1 population, and might reflect a higher degree of interspecific competition among carnivorans at Batallones-3. The presence in the Batallones-3 community of the ursid *Indarctos arctoides* and the thaumastocyonine *Thaumastocyon* sp., two very large carnivorans absent in Batallones-1, could have dramatically increased the levels of competition that *M. aphanistus* experienced in relation to the Batallones-1 community. The estimated body weight of the largest *I. arctoides* specimens is 254 kg (Abella, 2011) and that of *Thaumastocyon* would have been similar to that of the Middle Miocene *Amphicyon major*, which reached 223 kg (Figueirido et al., 2011). Given their body size, it is possible that these carnivorans were kleptoparasites on the kills of *M. aphanistus*, thus favoring a faster consumption of prey. The dentition of *I. arctoides* indicates an omnivorous diet (Viranta, 2004), but this species probably became more carnivorous during droughts, as observed in extant large omnivorous carnivorans in the lean season (Van Valkenburgh, 1989; Viranta, 2004). Thus, during dry periods, when carnivorans were more easily trapped in the Batallones traps due to the scarcity of both food and water, large specimens of *I. arctoides* would have been tempted to dispute carcasses defended by one or few individuals of *M. aphanistus*. The enigmatic *Thaumastocyon* does show a hypercarnivorous dentition, and although less abundant in the site than *M. aphanistus* or *I. arctoides*, it would have been also a serious opponent for both species. In contrast, in the Batallones-1 ecosystem, no other carnivore could have challenged an adult *M. aphanistus*, because the other large predator, the amphicyonid *Magericyon anceps*, had a considerably smaller body size than this felid. Nevertheless, its dentition shows markedly hypercarnivorous features, including moderately flattened upper canines (Peigné et al., 2008), so it is possible that both *M. aphanistus* and *Ma.*

anceps developed some kind of mutual avoidance, with the later species more likely to avoid encounters with the larger felid.

In summary, the observed paleoecological differences between the carnivoran communities from Batallones-1 and Batallones-3 fit well with the observed set of changes in the later populations of *M. aphanistus*, but a study of the postcranial remains of this species will likely shed more light on this issue.

LITERATURE CITED

Abella, J. 2011. *Indarctos arctoides* Depéret, 1895 (Carnivora, Mammalia) del yacimiento vallesiense de Batallones 3 (cuenca de Madrid). Ph.D. dissertation, Facultad de Ciencias, Universidad Autónoma de Madrid, Madrid, Spain, 403 pp.

Abella, J., M. S. Domingo, A. Valenciano, P. Montoya, and J. Morales. 2011. La asociación de carnívoros de Batallones-3, Mioceno superior del Cerro de los Batallones, cuenca de Madrid. Paleontologia i evoluciò, Memoria especial 5:21–24.

Alberdi, M. T., and F. P. Bonadonna. 1990. Climatic changes and presence of *Hipparion* in the Mediterranean area. Paléobiologie Continentale 17:281–290.

Alcalá, L. 1994. Macromamíferos neógenos de la fosa de Alfambra-Teruel. Instituto de Estudios Turolenses, Museo Nacional de Ciencias Naturales–CSIC, Teruel, Madrid, 554 pp.

Alderton, D. 1998. Wild Cats of the World. Blandford, London, 192 pp.

Antón, M., and J. Morales. 2000. Inferencias paleoecológicas de la asociación de carnívoros del yacimiento de Cerro Batallones; pp. 109–201 in J. Morales, M. Nieto, L. Amezua, S. Fraile, E. Gómez, E. Herráez, P. Peláez-Campomanes, M. J. Salesa, I. M. Sánchez, and D. Soria (eds.), Patrimonio Paleontológico de la Comunidad de Madrid. Serie "Arqueología, Paleontología y Etnografía," Volume 6. Comunidad de Madrid, Madrid.

Antón, M., M. J. Salesa, J. Morales, and A. Turner. 2004. First known complete skulls of the scimitar-toothed cat *Machairodus aphanistus* (Felidae, Carnivora) from the Spanish Late Miocene site of Batallones-1. Journal of Vertebrate Paleontology 24:957–969.

Bailey, T. N. 1993. The African Leopard: Ecology and Behavior of a Solitary Felid. Biology and Resource Management in the Tropics Series. Columbia University Press, New York, 429 pp.

Barone, R. 2010. Anatomie Comparée des Mammifères Domestiques, tome 1, Ostéologie, fifth edition. Éditions Vigot, Paris, 761 pp.

Bernor, R. L., J. Kovar-Eder, J. P. Suc, and H. Tobien. 1990. A contribution to the evolutionary history of European Late Miocene age hipparionines (Mammalia: Equidae). Paléobiologie Continentale 17:291–309.

Bertram, B. C. B. 1979. Serengeti predators and their social systems; pp. 221–248 in A. R. E. Sinclair and M. Norton-Griffiths (eds.), Serengeti, Dynamics of an Ecosystem. University of Chicago Press, Chicago, Illinois.

Bothma, J., and C. Walker. 1999. Larger Carnivores of the African Savannas. Springer-Verlag, Berlin, 274 pp.

Bowdich, T. E. 1821. An Analysis of the Natural Classifications of Mammalia for use of Students and Travellers. J. Smith, Paris, 115 pp.

Calvo, J. P., J. P., Pozo, M., Silva, P. G., and J. Morales. 2013. Pattern of sedimentary infilling of fossil mammal traps formed in pseudokarst

at Cerro de los Batallones, Madrid Basin, central Spain. Sedimentology 60:1681–1708.

de Beaumont, G. 1975. Recherches sur les Félidés (Mammifères, Carnivores) du Pliocène inférieur des Sables à *Dinotherium* des environs d'Eppelsheim (Rheinhessen). Archives des Sciences, Genève 28:369–405.

Emerson, S., and L. Radinsky. 1980. Functional analysis of sabertooth cranial morphology. Paleobiology 6:441–446.

Figueirido, B., J. A. Pérez-Claros, R. M. Hunt Jr., and P. Palmqvist. 2011. Body mass estimation in amphicyonid carnivoran mammals: a multiple regression approach from the skull and skeleton. Acta Palaeontologica Polonica 56:225–246.

Fischer, G. 1817. Adversaria zoologica. Mémoires de la Société Impériale des Naturalistes de Moscou 5:357–472.

Forstén, A. M. 1991. Size trends in Holarctic Anchitherines (Mammalia, Equidae). Journal of Paleontology 65:147–159.

Gill, T. 1872. Arrangement of the families of mammals with analytical tables. Smithsonian Miscellaneous Collections 11:1–98.

International Committee on Veterinary Gross Anatomical Nomenclature. 2005. Nomina Anatomica Veterinaria. Editorial Committee of the ICVGAN, Hannover, Columbia, Gent, Sapporo, 190 pp.

Kaup, J. J. 1833. Description d'Ossements Fossiles de Mammifères Inconnus Jusqu'á à-Présent, qui se Trouvent au Muséum Grand-Ducal de Darmstadt. Carnassiers Fossiles. J. G. Heyer, libraire-éditeur, Darmstadt.

Kretzoi, M. 1929. Materialen zur phylogenetischen klassifikation der Aeluroideen. 10th International Zoological Congress, Budapest 1927:1293–1355.

Kretzoi, N. 1945. Bemerkungen über das Raubtiersystem. Annales Historico-Naturales Musei Nationalis Hungarici 38:59–83.

Linnaeus, C. 1758. Systema naturae, per regna tria naturae, secundum classes, ordines, genera, species, cum characteribus, differentiis, synonymis, locis. 10th edition. Laurentii Salvil, Stockholm, 1384 pp.

López-Antoñanzas, R., P. Peláez-Campomanes, M. A. Álvarez-Sierra, and I. García-Paredes. 2010. New species of *Hispanomys* (Rodentia, Cricetodontinae) from the Upper Miocene of Batallones (Madrid, Spain). Zoological Journal of the Linnean Society 160:725–747.

Morlo, M. 1997. Die Raubtiere (Mammalia, Carnivora) aus dem Turolium von Dorn-Dürkheim 1 (Rheinhessen). Teil 1: Mustelida, Hyaenidae, Percrocutidae, Felidae. Courier Forschungs-Institut Senckenberg 197:11–47.

Morales, J., M. Pozo, P. G., Silva, M. S., Domingo, R., López-Antoñanzas, M. A. Álvarez Sierra, M. Antón, C. Martín Escorza, V. Quiralte, M. J. Salesa, I. M. Sánchez, B. Azanza, J. P. Calvo, P. Carrasco, I. García-Paredes, F. Knoll, M. Hernández Fernández, L. van den Hoek Ostende, L. Merino, A. J. van der Meulen, P. Montoya, S. Peigné, P. Peláez-Campomanes, A. Sánchez-Marco, A. Turner, J. Abella, G. M. Alcalde, M. Andrés, D. De Miguel, J. L. Cantalapiedra, S. Fraile, B. A. García Yelo, A. R. Gómez Cano, P. López Guerrero, A. Oliver Pérez, and G. Siliceo. 2008. El sistema de yacimientos de mamíferos miocenos del Cerro de los Batallones, Cuenca de Madrid: estado actual y perspectivas; pp. 41–117 in J. Esteve and G. Meléndez-Hevia (eds.), Palaeontologica Nova. Publicaciones del Seminario de Paleontología de Zaragoza, Zaragoza, Spain.

Morse, D. H. 1974. Niche breadth as a function of social dominance. American Naturalist 108:808–830.

Peigné, S., M. J. Salesa, M. Antón, and J. Morales. 2008. A new amphicyonine (Carnivora: Amphicyonidae) from the upper Miocene of Batallones-1, Madrid, Spain. Palaeontology 51:943–965.

Peigné, S., L. de Bonis, A. Likius, H. Taïsso Mackaye, P. Vignaud, and M. Brunet. 2005. A new machairodontine (Carnivora, Felidae) from the Late Miocene hominid locality of TM 266, Toros-Menalla, Chad. Comptes Rendus Palevol 4:243–253.

Plavcan, J. M. 1994. Comparison of four simple methods for estimating sexual dimorphism. American Journal of Physical Anthropology 94:465–476.

Pozo, M., and J. P. Calvo. 2004. Mineralogía y geoquímica isotópica de facies carbonáticas del cerro de los Batallones (Cuenca de Madrid). Implicaciones paleoambientales. Macla 2:31–32.

Roussiakis, S. J. 2002. Musteloids and feloids (Mammalia, Carnivora) from the lateMiocene locality of Pikermi (Attica, Greece). Geobios 35:699–719.

Salesa, M. J. 2002. Estudio anatómico, biomecánico, paleoecológico y filogenético de *Paramachairodus ogygia* (Kaup, 1832) Pilgrim, 1913 (Felidae, Machairodontinae) del yacimiento vallesiense (Mioceno superior) de Batallones-1 (Torrejón de Velasco, Madrid). Ph.D. dissertation, Facultad de Ciencias Biológicas, Universidad Complutense de Madrid, Madrid, Spain, 371 pp.

Salesa, M. J., M. Antón, J. Morales, and S. Peigné. 2012. Systematics and phylogeny of the small felines (Carnivora, Felidae) from the late Miocene of Europe: a new species of Felinae from the Vallesian of Batallones (MN 10, Madrid, Spain). Journal of Systematic Palaeontology 10:87–102.

Salesa, M. J., M. Antón, A. Turner, and J. Morales. 2006. Inferred behaviour and ecology of the primitive sabretoothed cat *Paramachairodus ogygia* (Felidae, Machairodontinae) from the Late Miocene of Spain. Journal of Zoology 268:243–254.

Salesa, M. J., M. Antón, A. Turner, L. Alcalá, P. Montoya, and J. Morales. 2010. Systematic revision of the Late Miocene sabretoothed felid *Paramachaerodus* in Spain. Palaeontology 53:1369–1391.

Sardella, R., and L. Werdelin. 2007. *Amphimachairodus* (Felidae, Mammalia) from Sahabi (latest Miocene-Earliest Pliocene, Libya), with a review of African Miocene Machairodontinae. Rivista Italiana di Paleontologia e Stratigrafia 113:67–77.

Schaller, G. B. 1972. The Serengueti Lion. University of Chicago Press, Chicago, Illinois, 504 pp.

Seidensticker, J. 1976. On the ecological separation between tigers and leopards. Biotropica 8:225–234.

Siliceo, G., M. J. Salesa, M. Antón, and J. Morales. 2011. Comparative study of two populations of the sabretoothed felid *Promegantereon ogygia* (Felidae, Machairodontinae) from Batallones-1 and Batallones-3 sites (Late Miocene, MN 10, Torrejón de Velasco, Madrid, Spain). Journal of Vertebrate Paleontology 31(6, Supplement):195.

Sotnikova, M. V. 1992. A new species of *Machairodus* from the Late Miocene Kalmakpai locality in eastern Kazakhastan (USSR). Annales Zoologici Fennici 28:361–369.

Turner, A., M. Antón, M. J. Salesa, and J. Morales. 2011. Changing ideas about the evolution and functional morphology of Machairodontine felids. Estudios Geológicos, 67:255–276.

Valenciano, A., J. Abella, O. Sanisidro, M. A. Álvarez-Sierra, and J. Morales. 2012. A complete skull and mandible of *Eomellivora piveteaui* Ozansoy, 1965 (Carnivora, Mammalia) from Batallones-3 (MN 10), Upper Miocene (Madrid, Spain); pp. 267–270 in R. Royo-Torres, F. Gascó, and L. Alcalá (coordinators), 10th Annual Meeting of the European Association of Vertebrate Palaeontologists, Teruel, 20–23 June 2012. ¡Fundamental! 20.

Van der Made, J., and T. S. Hussain. 1989. *Microstonyx major* (Suidae, Artiodactyla) from the type area of toe Nagriformation, Siwalik group, Pakistan. Estudios Geológicos 45:409–416.

Van Valkenburgh, B. 1989. Carnivore dental adaptations and diet: a study of trophic diversity within guilds; pp. 410–436 in J. L. Gittleman (ed.), Carnivore Behavior, Ecology, and Evolution, Volume 1. Cornell University Press, Ithaca, New York.

Van Valkenburgh, B., and T. Sacco. 2002. Sexual dimorphism, social behavior, and intrasexual competition in large Pleistocene carnivorans. Journal of Vertebrate Paleontology 22:164–169.

Viranta, S. 2004. Habitat preferences of European Middle Miocene omnivorous ursids. Acta Palaeontologica Polonica 49:325–327.

White, J. A., H. G. McDonald, E. Anderson, and J. M. Soiset. 1984. Lava blisters as carnivore traps. Carnegie Museum of Natural History Special Publication 8:241–256.